

# A QCD Sum Rule Approach to the $s \rightarrow d\gamma$ Contribution to the $\Omega^- \rightarrow \Xi^- \gamma$ Radiative Decay

M. Nielsen, L.A. Barreiro, C.O. Escobar and R. Rosenfeld\*  
*Instituto de Física, Universidade de São Paulo*  
*Caixa Postal 66318 - 5389-970 São Paulo, S.P., Brazil*

## Abstract

QCD sum rules are used to calculate the contribution of short-distance single-quark transition  $s \rightarrow d\gamma$ , to the amplitudes of the hyperon radiative decay,  $\Omega^- \rightarrow \Xi^- \gamma$ . We re-evaluate the Wilson coefficient of the effective operator responsible for this transition. We obtain a branching ratio which is comparable to the unitarity limit.

PACS numbers: 11.55.Hx, 13.40.Hq, 14.20.Jn, 12.15.Ji

Typeset using REVTeX

---

\*Address after October 1<sup>st</sup>: Instituto de Física Teórica, Universidade Estadual Paulista, Rua Pamplona 145, 01405-900 São Paulo-SP, Brazil

## I. INTRODUCTION

Hyperon radiative decays constitute an interesting class of processes that has been studied intensively, both theoretically and experimentally, for the past 20 years. However, despite these efforts we still lack a global understanding of these processes [1].

Some of these decays may be sensitive to the  $s \rightarrow d\gamma$  transition, which tests the Standard Model at the one-loop level and is similar to the  $b \rightarrow s\gamma$  transition recently seen at Cornell which has generated a large amount of interest [2]. Therefore, it would be extremely interesting to obtain any experimental information on it. In this paper we re-examine the assertion [3] that the decay  $\Omega^- \rightarrow \Xi^-\gamma$  can provide a window to the  $s \rightarrow d\gamma$  transition. In the following we briefly review the arguments that led to this conclusion.

There are two distinct contributions to hyperon radiative decays, namely short- and long-distance contributions. In short-distance processes, the photon is emitted at a close distance (typically  $x \simeq 1/M_W$ ) from the weak interaction vertex whereas in long-distance processes ( $x \simeq$  confinement radius) one can separate the weak from the electromagnetic vertices.

At the quark-level, there are in general three types of contribution to hyperon radiative decays, as shown in Fig. 1. The first diagram (Fig.1a) corresponds to a W-exchange and is a long-distance process, whereas Fig. 1b (single-quark transition  $s \rightarrow d\gamma$ ) and Fig. 1c (penguin diagram) are short-distance processes.

It is known that the  $s \rightarrow d\gamma$  transition cannot be the dominant one in all hyperon decays [4]. This is to be expected since W-exchange is the main term in the  $\Delta S = 1$  effective Hamiltonian. However, there are two hyperon radiative decays, namely  $\Omega^- \rightarrow \Xi^-\gamma$  and  $\Xi^- \rightarrow \Sigma^-\gamma$ , where the quark content of the initial and final state baryons does not allow a W-exchange contribution. Therefore, only the  $s \rightarrow d\gamma$  and penguin diagrams contribute at the quark level to the decay.

Let us concentrate first on  $\Xi^- \rightarrow \Sigma^-\gamma$ . It has been shown [5] that the penguin contribution for this process is negligible. In Ref. [6], the  $s \rightarrow d\gamma$  contribution to the branching ratio was calculated to be  $BR^{s \rightarrow d\gamma}(\Xi^- \rightarrow \Sigma^-\gamma) = 1.8 \times 10^{-5}$ . However, although the W-exchange process does not contribute directly to  $\Xi^- \rightarrow \Sigma^-\gamma$ , it does contribute to  $\Xi^- \rightarrow \pi^-\Lambda$ , where the final state can then re-scatter as  $\pi^-\Lambda \rightarrow \Sigma^-\gamma$ . This long-distance contribution has been estimated as  $BR^{LD}(\Xi^- \rightarrow \Sigma^-\gamma) = 1.7 \times 10^{-4}$  [7], close to the experimental result  $BR^{Exp}(\Xi^- \rightarrow \Sigma^-\gamma) = (1.27 \pm 0.23) \times 10^{-4}$  [8].

This leaves us with the process  $\Omega^- \rightarrow \Xi^-\gamma$  as the only candidate for probing the  $s \rightarrow d\gamma$  transition in hyperon radiative decays. Let us summarize what is known about this process so far. There is an experimental upper limit determined recently [9]:

$$BR^{Exp.}(\Omega^- \rightarrow \Xi^-\gamma) < 4.6 \times 10^{-4}. \quad (1.1)$$

This is well above the unitarity limit [7] :

$$BR^{Unitarity}(\Omega^- \rightarrow \Xi^-\gamma) > 0.8 \times 10^{-5}. \quad (1.2)$$

The penguin contribution has been estimated as [5] :

$$BR^{Penguin}(\Omega^- \rightarrow \Xi^-\gamma) \simeq 5 \times 10^{-6}. \quad (1.3)$$

Kogan and Shifman [7] have also calculated the long-distance contribution from the dominant  $\Xi^0\pi^-$  intermediate state as :

$$BR^{LD}(\Omega^- \rightarrow \Xi^- \gamma) = (1-1.5) \times 10^{-5}. \quad (1.4)$$

The contribution from the single-quark  $s \rightarrow d\gamma$  transition has been re-evaluated recently [10] yielding :

$$BR^{s \rightarrow d\gamma}(\Omega^- \rightarrow \Xi^- \gamma) = 8.0 \times 10^{-7} \quad (1.5)$$

This result corrects a previous calculation [3], where it was claimed that the single quark transition should be the dominant contribution to the  $\Omega^-$  radiative decay. Both calculations [10,3] were based on estimating the hadronic matrix element of the effective operator describing the single-quark transition, using SU(6) quark-model wave functions and assuming unit overlap.

Due to the importance of this process, we believe that a more reliable estimate of the single-quark  $s \rightarrow d\gamma$  contribution to the radiative decay  $\Omega^- \rightarrow \Xi^- \gamma$  is in order. This is the purpose of the present work, where we perform a calculation of the same matrix element using the well known technique of QCD sum rules [11].

The QCD sum rule approach was successfully applied to the  $\Sigma^+ \rightarrow p\gamma$  decay by Balitisky and collaborators [12], who calculated in this way the dominant W-exchange. QCD sum-rules were also employed before for the calculation of the single-quark contribution [13] to the  $\Sigma^+$  and  $\Xi^-$  radiative decays. Although the single quark transition is not the dominant contribution in these decays, the calculation exposed the role of non-perturbative corrections which alter the naive picture of the single-quark transition in a major way: it showed that it is not a good approximation to assume a unity overlap for the quark-model wave functions.

This paper is organized as follows. Section II discusses the effective operator for the  $s \rightarrow d\gamma$  transition. In Section III we derive the sum rules and in Section IV we present the results and conclusions.

## II. THE EFFECTIVE OPERATOR FOR $S \rightarrow D\gamma$ TRANSITION

We are interested in computing the contribution of the quark level  $s \rightarrow d\gamma$  transition to the radiative decay  $\Omega \rightarrow \Xi\gamma$ . This transition does not occur at tree-level in the Standard Model. Hence, it could in principle provide a good test to the Standard Model at the 1-loop level, being sensitive also to new Physics.

The effective hamiltonian (with the heavy quarks  $c, b$  and  $t$  as well as electroweak gauge bosons integrated out ) that describes  $|\Delta S = 1|$  transitions is given by :

$$\mathcal{H}_{\text{eff}}^{|\Delta S=1|} = \frac{-4G_F}{\sqrt{2}} \lambda_u \sum_{k=1}^8 c_k(\mu) \mathcal{O}_k(\mu), \quad (2.1)$$

where  $G_F$  is the Fermi constant, and we use the notation  $\lambda_i$  to denote the following product of elements of the Cabibbo-Kobayashi-Maskawa (CKM) matrix,  $\lambda_i = V_{si}V_{id}^*$ . The Wilson coefficients  $c_k$  can be computed perturbatively and  $\{\mathcal{O}_k\}$  is a complete set of operators written as:

$$\begin{aligned}
\mathcal{O}_1 &= (\bar{u}_\alpha \gamma_\mu P_L s_\beta) (\bar{d}_\beta \gamma^\mu P_L u_\alpha) \\
\mathcal{O}_2 &= (\bar{u}_\alpha \gamma_\mu P_L s_\alpha) (\bar{d}_\beta \gamma^\mu P_L u_\beta) \\
\mathcal{O}_3 &= (\bar{d}_\alpha \gamma_\mu P_L s_\alpha) \sum_{q=u,d,s} (\bar{q}_\beta \gamma^\mu P_L q_\beta) \\
\mathcal{O}_4 &= (\bar{d}_\alpha \gamma_\mu P_L s_\beta) \sum_{q=u,d,s} (\bar{q}_\beta \gamma^\mu P_L q_\alpha) \\
\mathcal{O}_5 &= (\bar{d}_\alpha \gamma_\mu P_L s_\alpha) \sum_{q=u,d,s} (\bar{q}_\beta \gamma^\mu P_R q_\beta) \\
\mathcal{O}_6 &= (\bar{d}_\alpha \gamma_\mu P_L s_\beta) \sum_{q=u,d,s} (\bar{q}_\beta \gamma^\mu P_R q_\alpha) \\
\mathcal{O}_7 &= \frac{ie}{16\pi^2} m_s (\bar{d}_\alpha \sigma_{\mu\nu} P_R s_\alpha) F^{\mu\nu} \\
\mathcal{O}_8 &= \frac{ig_s}{16\pi^2} m_s (\bar{d}_\alpha \sigma_{\mu\nu} T_{\alpha\beta}^a P_R s_\beta) G^{a\mu\nu}, \tag{2.2}
\end{aligned}$$

where  $P_{L,R} = \frac{1}{2}(1 \mp \gamma_5)$ ,  $\sigma_{\mu\nu} = i[\gamma_\mu, \gamma_\nu]/2$ ;  $F^{\mu\nu}$  and  $G^{a\mu\nu}$  are the electromagnetic and color field tensors respectively.

We are interested in the Wilson coefficient  $c_7(\mu = m_s)$ , which controls the short distance contribution to the process  $s \rightarrow d\gamma$ .

The Wilson coefficients are first computed at the scale  $\mu = M_W$  in zeroth order in QCD. QCD corrections are included by evolving these coefficients down to  $\mu = m_s$  using the renormalization group equations. This evolution is accomplished in three steps. Schematically one has :

$$c_k(\mu = m_s) = U_{kl}^3(m_s, m_c) U_{ln}^4(m_c, m_b) U_{nm}^5(m_b, M_W) c_m(M_W). \tag{2.3}$$

The evolution matrix with  $f$  active quark flavors in the leading logarithmic approximation can be written as [14] :

$$U^f(m_1, m_2) = VTV^{-1}, \tag{2.4}$$

where  $V$  is a matrix that diagonalizes the transpose of the  $8 \times 8$  anomalous dimension matrix  $\gamma$  :

$$\gamma_D = V^{-1}\gamma V, \tag{2.5}$$

and  $T$  is a diagonal matrix with elements given by :

$$T_{ii} = \left[ \frac{\alpha_s(m_2)}{\alpha_s(m_1)} \right]^{(\gamma_D)_{ii}/2\beta_0}, \tag{2.6}$$

where  $\beta_0 = 11 - 2f/3$  and in this approximation the running of the strong coupling constant is described by :

$$\alpha_s(m_2) = \frac{\alpha_s(m_1)}{1 - \frac{\beta_0}{2\pi} \alpha_s(m_1) \ln(m_1/m_2)}. \quad (2.7)$$

We now turn to a discussion of the initial conditions. Due to our choice of factoring out  $\lambda_u$  in eq.(2.1), we have:

$$c_2(M_W) = 1 \quad , \quad c_{1,3-6}(M_W) = 0. \quad (2.8)$$

The values for  $c_7$  and  $c_8$  at  $\mu = M_W$  are given in terms of functions arising from one-loop diagrams with an external photon and a gluon respectively [15,16]. These function  $F_2(x_i)$  and  $D(x_i)$ , where  $x_i = m_i^2/M_W^2$  and  $m_i$  is the mass of the quark running in the loop, are given by:

$$F_2(x) = Q \left[ \frac{x^3 - 5x^2 - 2x}{4(x-1)^3} + \frac{3x^2 \ln(x)}{2(x-1)^4} \right] + \frac{2x^3 + 5x^2 - x}{4(x-1)^3} - \frac{3x^3 \ln(x)}{2(x-1)^4}; \quad (2.9)$$

$$D(x) = \frac{x^3 - 5x^2 - 2x}{4(x-1)^3} + \frac{3x^2 \ln(x)}{2(x-1)^4}, \quad (2.10)$$

where  $Q$  is the charge of the internal quark.

In table 1 we show the contributions to  $F_2$  from the different internal quarks and its product with the relevant CKM matrix elements. We use the following values for the quark masses and  $\lambda_i$ :  $m_t = 175$  GeV,  $m_c = 1.5$  GeV,  $m_u = 5$  MeV,  $\lambda_u = 0.21$ ,  $\lambda_c = -0.21$  and  $\lambda_t = -(1.2 - 7.2) \times 10^{-4}$ , where the CKM elements were obtained from the standard parametrization of the Particle Data Book neglecting CP violation, that is taking  $\delta_{13} = 0$ .

From this table we see that, as opposed to the  $b \rightarrow s\gamma$  case, the top quark contribution is not the dominant one for  $s \rightarrow d\gamma$  and we must take into account both  $t$ - and  $c$ - quarks in computing the initial values for  $c_7$  and  $c_8$ , which are given by :

$$c_7(M_W) = \frac{-1}{2} \left( \frac{\lambda_t}{\lambda_u} F_2(x_t) + \frac{\lambda_c}{\lambda_u} F_2(x_c) \right); \quad (2.11)$$

$$c_8(M_W) = \frac{-1}{2} \left( \frac{\lambda_t}{\lambda_u} D(x_t) + \frac{\lambda_c}{\lambda_u} D(x_c) \right). \quad (2.12)$$

In order to compute the evolution matrix we use the anomalous dimension matrix given in ref. [14] and  $\alpha_s(M_W) = 0.124$ . However, from eq.(2.7) one would get a value for  $\alpha_s(m_s) > 1$ , since for consistency with the leading-log anomalous dimension matrix we have to compute the running of  $\alpha_s$  in one-loop only. In this case we use  $\alpha_s(m_s) = 1$ . We find:

$$c_7(m_s) = -0.50c_2(M_W) + 0.27c_7(M_W) + 0.13c_8(M_W). \quad (2.13)$$

The numerical values for the initial conditions for  $c_7$  and  $c_8$  are:

$$c_7(M_W) = (2.1 - 7.7) \times 10^{-4} \quad , \quad c_8(M_W) = (1.4 - 4.2) \times 10^{-4}, \quad (2.14)$$

and from Eq.(2.13) we see that  $c_7(m_s)$  is insensitive to the the values of  $c_7(M_W)$  and  $c_8(M_W)$ , being dominated by  $c_2(M_W)$ . This result is in contrast to what happens in the  $b \rightarrow s\gamma$  case. It can be understood since in the  $s \rightarrow d\gamma$  case we have  $c_2(M_W) \propto \lambda_u$  and  $c_{7,8}(M_W)$  is effectively proportional to  $\lambda_t$  with  $\lambda_t \ll \lambda_u$ ; in the  $b \rightarrow s\gamma$  case, one has  $c_2(M_W) \propto |V_{bc}V_{cs}^*| \simeq |V_{bt}V_{ts}^*| \propto c_{7,8}(M_W)$ .

Unfortunately, Physics beyond the Standard Model would contribute mostly to  $c_{7,8}(M_W)$  and from our calculation we see that unless the modification implies in an increase of  $c_{7,8}(M_W)$  by roughly four orders of magnitude, no significant contribution will be made to the  $s \rightarrow d\gamma$  process.

Using equations (2.2), (2.8) and (2.13) we arrive at the main result of this section:

$$\mathcal{H}_{\text{eff}}^{s \rightarrow d\gamma} = \frac{-4G_F}{\sqrt{2}} \lambda_u c_7(m_s) \mathcal{O}_7 = (0.28) \frac{ieG_F}{16\pi^2} m_s (\bar{d}_\alpha \sigma_{\mu\nu} P_R s_\alpha) F^{\mu\nu} . \quad (2.15)$$

### III. QCD SUM RULES

The subject of this section is the evaluation of the  $s \rightarrow d\gamma$  contribution to the four multipole amplitudes that appear in the transition matrix related to the radiative decay  $\Omega^- \rightarrow \Xi^- \gamma$ , using a QCD sum rule approach.

#### A. Formalism

We start with the three-point correlation function

$$\Pi_\mu(Q_i, Q_f) = -i \int d^4x d^4y e^{iQ_f y} e^{-iQ_i x} \langle 0 | T[\eta^{\Xi^-}(y) \mathcal{H}_{\text{eff}}^{s \rightarrow d\gamma}(0) \bar{\eta}_\mu^\Omega(x)] | 0 \rangle , \quad (3.1)$$

where  $\mathcal{H}_{\text{eff}}^{s \rightarrow d\gamma}$  is given by Eq.(2.15).

As usual, our goal is to make a match between the two representations of the correlation function (3.1) at a certain region  $Q_i^2 \sim 1 \text{ GeV}^2$ : the operator product expansion (OPE) in powers of  $Q_i^2$  and the phenomenological representation of the dispersion integrals. The basic idea, supported by ample successful applications, is that taking into account only the first few terms in the  $Q_i^2$  expansion, complemented by rather simple assumptions for the higher mass contributions to the dispersion relation, will already provide a good estimate to the amplitudes of interest.

The  $\Omega^-$  and  $\Xi^-$  interpolating fields are given by [18]

$$\eta^{\Xi^-}(x) = -\epsilon_{abc} \left( s_a^T(x) C \gamma_\mu s_b(x) \right) \gamma_5 \gamma^\mu d_c(x) , \quad (3.2)$$

$$\eta_\mu^{\Omega^-}(x) = \epsilon_{abc} \left( s_a^T(x) C \gamma_\mu s_b(x) \right) s_c(x) . \quad (3.3)$$

With these definitions and working at leading order in perturbation theory we obtain for the T product appearing in Eq.(3.1)

$$\begin{aligned} \langle 0 | T[\eta^{\Xi}(y) \mathcal{H}_{eff}^{s \rightarrow d\gamma}(0) \bar{\eta}_{\mu}^{\Omega}(x)] | 0 \rangle &= \frac{-ieG_F}{16\pi^2} 0.28 m_s \epsilon_{abc} \epsilon_{a'b'c'} F^{\alpha\beta} \gamma_5 \gamma^{\nu} S_{ce}^d(y) (1 + \gamma_5) \sigma_{\alpha\beta} S_{e'c'}^s(-x) \times \\ &\left\{ \text{tr}[S_{bb'}^s(y-x) \gamma_{\mu} C(S_{aa'}^s(y-x))^T C \gamma_{\nu}] + 2\gamma_{\mu} C(S_{aa'}^s(y-x))^T C \gamma_{\nu} S_{bb'}^s(y-x) \right\}, \end{aligned} \quad (3.4)$$

where the coordinate-space quark propagator in the presence of the quark condensate takes the following form [18,19]

$$S_{ab}^q(x) = \langle 0 | T[q_a(x) \bar{q}_b(0)] | 0 \rangle = \frac{i\delta_{ab} \not{x}}{2\pi^2 x^4} - \frac{\delta_{ab} m_q}{4\pi^2 x^2} - \frac{\delta_{ab}}{12} \langle \bar{q}q \rangle + \frac{i\delta_{ab}}{48} m_q \langle \bar{q}q \rangle \not{x} + \dots \quad (3.5)$$

The amplitude  $\Pi_{\mu}(Q_i, Q_f)$  includes a lot of different non-trivial Lorentz structures. For each one of these structures,  $\Pi_k(Q_i^2, Q_f^2)$ , we can write a double dispersion representation of the form

$$\Pi_k(Q_i^2, Q_f^2) = \frac{1}{\pi^2} \int_0^{\infty} ds_1 \int_0^{\infty} ds_2 \frac{\rho_k(s_1, s_2)}{(s_1 + Q_f^2)(s_2 + Q_i^2)} + \dots, \quad (3.6)$$

where the ellipsis represents subtractions polynomials in  $Q_i^2$  and  $Q_f^2$ , which will vanish under the double Borel transform [20], which is a straightforward generalization of that used in Ref. [11]. Applying the double Borel transform to Eq.(3.6) gives

$$\Pi_k(M_1^2, M_2^2) = \frac{1}{\pi^2} \int_0^{\infty} ds_1 \int_0^{\infty} ds_2 \rho_k(s_1, s_2) e^{-s_1/M_1^2} e^{-s_2/M_2^2}. \quad (3.7)$$

In the phenomenological side the various Lorentz structures can be obtained from the consideration of the  $\Omega$  and  $\Xi$  contribution to the dispersion sum rule

$$\langle 0 | \eta^{\Xi} | \Xi(Q_f) \rangle \langle \Xi(Q_f) \gamma | \mathcal{H}_{eff}^{s \rightarrow d\gamma} | \Omega(Q_i) \rangle \langle \Omega(Q_i) | \bar{\eta}_{\mu}^{\Omega} | 0 \rangle, \quad (3.8)$$

where the most general, gauge invariant form for the amplitude of the  $\Omega^- \rightarrow \Xi^- \gamma$  decay is given by [3]

$$\begin{aligned} M(\Omega^- \rightarrow \Xi^- \gamma) &= \langle \Xi(Q_f) \gamma | \mathcal{H}_{eff}^{s \rightarrow d\gamma} | \Omega(Q_i) \rangle = ieG_F \bar{u}^{(\Xi)}(Q_f) [(a_1 + \gamma_5 a_2) (\not{q} g^{\mu\nu} - \gamma^{\mu} q^{\nu}) \\ &+ (b_1 + \gamma_5 b_2) (Q_i \cdot q g^{\mu\nu} - Q_i^{\mu} q^{\nu}) / M_{\Omega}] u_{\nu}^{(\Omega)}(Q_i) \epsilon_{\mu}, \end{aligned} \quad (3.9)$$

where  $q = Q_f - Q_i$ ,  $\epsilon_{\mu}$  is the polarization of the photon, and  $a_1$ ,  $a_2$ ,  $b_1$  and  $b_2$  are the four amplitudes we want to evaluate. The other matrix elements contained in Eq.(3.8) are of the form

$$\langle 0 | \eta^{\Xi} | \Xi(Q_f) \rangle = \lambda_{\Xi} u^{(\Xi)}(Q_f), \quad (3.10)$$

$$\langle \Omega(Q_i) | \bar{\eta}_{\mu}^{\Omega} | 0 \rangle = \lambda_{\Omega} \bar{u}_{\mu}^{(\Omega)}(Q_i), \quad (3.11)$$

where  $u_{\mu}(p)$  is a Rarita-Schwinger spin-vector satisfying

$$u_{\mu}^{(\Omega)}(p) \bar{u}_{\nu}^{(\Omega)}(p) = - \left( g^{\mu\nu} - \frac{1}{3} \gamma_{\mu} \gamma_{\nu} - \frac{2}{3M_{\Omega}^2} p_{\mu} p_{\nu} + \frac{\gamma_{\mu} p_{\nu} - \gamma_{\nu} p_{\mu}}{3M_{\Omega}} \right) (\not{p} + M_{\Omega}), \quad (3.12)$$

$u(p)$  is a Dirac spinor and  $\lambda_\Xi$ ,  $\lambda_\Omega$  are the couplings of the currents with the respective hadronic states.

Saturating the correlation function Eq.(3.1) with  $\Omega$  and  $\Xi$  intermediate states, and using Eqs.(3.8), (3.9), (3.10), (3.11) and (3.12) we get

$$\begin{aligned} \Pi_\mu^{(phen)}(Q_i, Q_f) = & -ieG_F\lambda_\Xi\lambda_\Omega\frac{(\not{q} + \not{Q}_i + M_\Xi)}{Q_f^2 + M_\Xi^2} \left[ (a_1 + \gamma_5 a_2)(\not{q}\epsilon^\beta - \not{q}^\beta) + (b_1 + \gamma_5 b_2) \times \right. \\ & \left. (Q_i \cdot q\epsilon^\beta - Q_i \cdot \epsilon q^\beta) \frac{1}{M_\Omega} \right] \left( g_{\beta\mu} - \frac{1}{3}\gamma_\beta\gamma_\mu - \frac{2}{3M_\Omega^2}Q_\beta^i Q_\mu^i + \frac{\gamma_\beta Q_\mu^i - \gamma_\mu Q_\beta^i}{3M_\Omega} \right) \frac{(Q_i + M_\Omega)}{Q_i^2 + M_\Omega^2}. \end{aligned} \quad (3.13)$$

In this work we will derive sum rules for the Lorentz structures:

$$a : \not{q}(a_1 + \gamma_5 a_2)\sigma_{\alpha\beta}\gamma_\mu Q_i \epsilon^\alpha q^\beta, \quad (3.14)$$

$$b : \not{q}(b_1 + \gamma_5 b_2)(Q_i \cdot q\epsilon_\mu - Q_i \cdot \epsilon q_\mu). \quad (3.15)$$

This choice is based on the fact that the structure a gets perturbative contribution (which is very important in the case of double dispersion relation analysed here [20]) as well as power corrections contributions, and the structure b is the only one that contributes solely to the amplitudes  $b_1$  and  $b_2$ . Furthermore, as we will show, both sum rules are very stable as a function of the Borel masses.

For the continuum contribution we adopt the standard form of Ref. [20], which completes our parametrization of the spectral density  $\rho_k$ :

$$\begin{aligned} \frac{1}{\pi^2}\rho_a(s_1, s_2) = & \frac{-2}{3}eG_F\lambda_\Xi\lambda_\Omega\delta(s_1 - M_\Xi^2)\delta(s_2 - M_\Omega^2) \\ & + \theta(s_1 - s_\Xi)\theta(s_2 - s_\Omega)\rho_a^{(0)}(s_1, s_2), \end{aligned} \quad (3.16)$$

$$\begin{aligned} \frac{1}{\pi^2}\rho_b(s_1, s_2) = & -ieG_F\lambda_\Xi\lambda_\Omega\delta(s_1 - M_\Xi^2)\delta(s_2 - M_\Omega^2) \\ & + \theta(s_1 - s_\Xi)\theta(s_2 - s_\Omega)\rho_b^{(0)}(s_1, s_2), \end{aligned} \quad (3.17)$$

where  $s_\Xi$ ,  $s_\Omega$  are, respectively, the continuum threshold of the  $\Xi$  and  $\Omega$  determined in the mass sum rules, and  $\rho_k^{(0)}(s_1, s_2)$  is the free-quark spectral function.

Let us now calculate the left-hand side of the sum rule Eq.(3.7) using the OPE. We shall consider only the diagrams shown in Fig.2. The perturbative contribution to the sum rule is shown in Fig.2a and is obtained by using only the first term in the right-hand side of Eq.(3.5) in Eq.(3.4). The resulting expressions for the two chosen structures are

$$\Pi_\mu^{(a)}(M_1^2, M_2^2) = \frac{-3eG_F 0.28m_s}{2^9\pi^6} \frac{M_1^6 M_2^6}{(M_1^2 + M_2^2)^3} \not{q}(1 - \gamma_5)\sigma_{\alpha\beta}\gamma_\mu Q_i \epsilon^\alpha q^\beta, \quad (3.18)$$

$$\Pi_\mu^{(b)}(M_1^2, M_2^2) = \frac{3ieG_F 0.28m_s}{2^8\pi^6} \frac{M_1^6 M_2^8}{(M_1^2 + M_2^2)^4} \not{q}(1 - \gamma_5)(Q_i \cdot q\epsilon_\mu - Q_i \cdot \epsilon q_\mu). \quad (3.19)$$

Noticing that Eq.(3.7) is the double Laplace transformation in  $1/M_i^2$ , the free-quark spectral function,  $\rho_k^{(0)}(s_1, s_2)$ , can be obtained from Eqs.(3.18) and (3.19) by applying the inverse transformation. It gives



$$\frac{1}{\pi^2}\rho_a^{(0)}(s_1, s_2) = \frac{-3eG_F 0.28m_s}{2^{10}\pi^6} s_1 s_2 \delta(s_1 - s_2), \quad (3.20)$$

$$\frac{1}{\pi^2}\rho_b(s_1, s_2) = \frac{-ieG_F 0.28m_s}{2^9\pi^6} s_2^3 \delta'(s_2 - s_1). \quad (3.21)$$

The next term in the OPE is determined by Figs.2b, c and d. The contribution of Fig.2d exactly cancels the contributions of Figs.2b and c for the structure b. The result of the three diagrams for the structure a is

$$\frac{5eG_F 0.28m_s}{2^6\pi^4} m_s \langle \bar{s}s \rangle \frac{M_1^2 M_2^2}{(M_1^2 + M_2^2)^2} \left[ M_2^2 + M_1^2 \ln \left( \frac{M_1^2 + M_2^2}{m_s^2} \right) \right] \not{q} (1 - \gamma_5) \sigma_{\alpha\beta} \gamma_\mu \not{Q}_i \epsilon^\alpha q^\beta. \quad (3.22)$$

The last diagram which we take into account is shown in Fig.2e. It does not give any contribution to the structure b and the contribution to the structure a is

$$\frac{-eG_F 0.28m_s}{12\pi^2} \langle \bar{s}s \rangle^2 \not{q} (1 - \gamma_5) \sigma_{\alpha\beta} \gamma_\mu \not{Q}_i \epsilon^\alpha q^\beta. \quad (3.23)$$

The gluon condensate is not taken into account because its contribution is suppressed relative to the operator  $m_q \langle \bar{q}q \rangle$  (which has the same dimension) by an extra loop factor  $1/16\pi^2$ .

In general, when a real photon is emitted, one has also to consider diagrams such as that in Figure 3, involving long distances in the photon channel. However, this diagram gives a negligible contribution, as it is proportional to the part of the photon wave function at long distances, involving quarks of different flavors [12,21]. Therefore, we do not consider it here.

Collecting all the obtained contributions, and transferring the continuum contribution to the OPE side, we arrive at the following representation to the amplitudes:

$$a_1 = -a_2 = \frac{3}{2\pi^2} \frac{e^{M_\Xi^2/M_1^2} e^{M_\Omega^2/M_2^2}}{\tilde{\lambda}_\Xi \tilde{\lambda}_\Omega} 0.28m_s \left[ \frac{3}{2^6} \int_0^{s_\Xi} ds_1 \int_0^{s_\Omega} ds_2 s_1 s_2 \delta(s_1 - s_2) e^{-s_1/M_1^2} e^{-s_2/M_2^2} \right. \\ \left. + \frac{5\pi^2}{16} m_s f a \frac{M_1^2 M_2^2}{(M_1^2 + M_2^2)^2} \left( M_2^2 + M_1^2 \ln \left( \frac{M_1^2 + M_2^2}{m_s^2} \right) \right) + \frac{1}{12} f^2 a^2 \right], \quad (3.24)$$

$$b_1 = -b_2 = \frac{1}{2^5\pi^2} \frac{e^{M_\Xi^2/M_1^2} e^{M_\Omega^2/M_2^2}}{\tilde{\lambda}_\Xi \tilde{\lambda}_\Omega} 0.28m_s \int_0^{s_\Xi} ds_1 \int_0^{s_\Omega} ds_2 s_2^3 \frac{d}{ds_2} (\delta(s_2 - s_1)) e^{-s_1/M_1^2} e^{-s_2/M_2^2}, \quad (3.25)$$

where  $\tilde{\lambda}_H = 4\pi^2 \lambda_H$ ,  $a = -4\pi^2 \langle \bar{q}q \rangle$ , and  $f = \langle \bar{s}s \rangle / \langle \bar{q}q \rangle$ .

## B. Sum Rule Analysis

The sum rules are sampled in the region of Borel mass,  $M^2$ , which have been identified as the fiducial region for the baryon mass sum rules [22]

$$1.4 \leq M_1^2 \leq 2.0 \text{ GeV}^2 \quad \text{for } \Xi, \quad (3.26)$$

$$2.4 \leq M_2^2 \leq 3.2 \text{ GeV}^2 \quad \text{for } \Omega. \quad (3.27)$$

The values used for  $\tilde{\lambda}_H$  and  $s_H$  are extracted from the respective mass sum rules analysed in the same region given above. For  $\Xi$  we get from Ref. [22]  $\tilde{\lambda}_\Xi \simeq 1.6\text{GeV}^3$  and  $s_\Xi = 3.6\text{GeV}^2$ . For  $\Omega$ , using the sum rules given in [23], we get  $\tilde{\lambda}_\Omega \simeq 3.8\text{GeV}^3$  and  $s_\Omega \simeq 7.5\text{GeV}^2$ . The value of the other parameters are [22]:  $a = 0.55\text{GeV}^3$ ,  $m_s = 150\text{MeV}$ ,  $f = 0.8$ ,  $M_\Xi = 1.32\text{GeV}$  and  $M_\Omega = 1.67\text{GeV}$ .

In Fig.4 we show the result obtained for  $a_1$  as a function of  $M_1^2$  for different values of  $M_2^2$ . One can see that  $a_1$  varies very slowly with  $M_1^2$  but not so slowly with  $M_2^2$ . In the Borel region considered the amplitude  $a_1$  change less than 20%. The same behaviour can be observed in Fig.5 where  $a_1$  is plotted as a function of  $M_2^2$  for different values of  $M_1^2$ .

For the amplitude  $b_1$  we get an even more stable result. As can be seen by Figs.6 and 7  $b_1$  varies slowly with  $M_2^2$  and with  $M_1^2$ . In the Borel region considered  $b_1$  changes less than 10%. Using  $M_1^2 = M_\Xi^2$  and  $M_2^2 = M_\Omega^2$  we get

$$a_1 = -a_2 \simeq 1.10\text{MeV}, \quad (3.28)$$

$$b_1 = -b_2 \simeq -0.58\text{MeV}. \quad (3.29)$$

#### IV. RESULTS AND CONCLUSIONS

Given the values of the form factors  $a_1, a_2, b_1, b_2$ , we can compute the decay width  $\Gamma(\Omega^- \rightarrow \Xi^- \gamma)$  [3]:

$$\Gamma(\Omega^- \rightarrow \Xi^- \gamma) = \frac{2}{3} \alpha G_F^2 q_0^3 H \quad (4.1)$$

where

$$q_0 = \frac{(M_\Omega^2 - M_\Xi^2)}{2M_\Omega} \quad (4.2)$$

is the photon energy in the  $\Omega$  rest frame and

$$H = \left[ \left(1 + \frac{p_\Omega \cdot p_\Xi}{M_\Omega^2}\right)(a_1^2 + a_2^2) + \left(\frac{p_\Omega \cdot p_\Xi}{M_\Omega^2}\right)(b_1^2 + b_2^2) + \right. \\ \left. \left(1 + \frac{p_\Omega \cdot p_\Xi}{M_\Omega^2}\right)(a_1 b_1 + a_2 b_2) + \frac{M_\Xi}{M_\Omega}(b_1^2 - b_2^2) + \frac{2M_\Xi}{M_\Omega}(a_1 b_1 - a_2 b_2) \right] \quad (4.3)$$

Using the values obtained in the last section we get:

$$\Gamma(\Omega^- \rightarrow \Xi^- \gamma) = 5.6 \times 10^{-11} \text{eV} \quad (4.4)$$

which results in a branching ratio

$$\text{BR}(\Omega^- \rightarrow \Xi^- \gamma) = 7.0 \times 10^{-6}. \quad (4.5)$$

As mentioned before, the penguin contributions to this decay were calculated using bag model matrix elements, for weak and electromagnetic transitions at baryon level, and standard penguin coefficients, yielding [5]:

$$\text{BR}^{Penguin}(\Omega^- \rightarrow \Xi^- \gamma) \sim 2 \times 10^{-3} (C_P/C_1)^2 \simeq 5 \times 10^{-6}, \quad (4.6)$$

where the ratio of the  $C_P/C_1$  coefficients of the QCD-corrected nonleptonic Hamiltonian is approximately  $1/20$  [11,25,26].

Our result suggests that the different contributions to the branching ratio  $BR(\Omega^- \rightarrow \Xi^- \gamma)$  arising from the single-quark  $s \rightarrow d\gamma$  transition, Eq.(4.5), the penguin diagram, Eq.(4.6), and the long distance process, Eq.(1.4), are all comparable. In order to separate the contributions from these different processes it may be necessary to study the asymmetry parameters of the decay. It is also worth mentioning that the result given in Ref. [10], Eq.(1.5), would be of the same order as our result, Eq.(4.5), had they used the same value of  $c_7(m_s)$  given here. In Ref. [10] they also estimated another class of long distance contributions to the  $\Omega^- \rightarrow \Xi^- \gamma$  decay, using the vector meson dominance approximation, and they found that it could possibly saturate the experimental upper bound. However, their long distance result is proportional to a quantum chromodynamics coefficient, whose direct estimate is not reliable since all the calculation is far from the perturbative regime. For this reason we chose to quote here only the more traditional long distance result given in Ref. [7].

Our result is roughly a factor of 60 below the experimental upper limit, Eq.(1.1), and it would be extremely interesting if new experiments could bring the upper limit down, since even adding all the contributions to this decay, one still gets a number that is at least one order of magnitude smaller than the experimental upper limit.

## V. ACKNOWLEDGMENTS

We would like to thank I.F. Albuquerque for useful discussions and for insisting on the relevance of the subject. R.R. would like to thank A. Ioannissian for useful correspondence. This work was partially supported by CNPq and FAPESP.

## REFERENCES

- [1] For a review, see J. Lach and P. Zenczykowski, preprint Fermilab-Pub-95/040, to be published in International Journal of Modern Physics A.
- [2] R. Ammar *et al.*, Phys. Rev. Lett. **71**, 674 (1993).
- [3] R. Safadi and P. Singer, Phys. Rev. **D37**, 697 (1988); **D42**, 1856E (1990); P. Singer, “Some Weak Hyperon Radiative Decays - A Possible Window to the  $s \rightarrow d\gamma$  Transition”, Essays in honor of M. Roos (M. Chaichian and J. Maalapi, eds.), p143 (1991).
- [4] F. Gilman and M.B. Wise, Phys. Rev. **D19**, 976 (1979).
- [5] S.G. Kamath, Nucl. Phys. **B198**, 61 (1982); J.O. Eeg, Z. Phys. **C21**, 253 (1984).
- [6] L. Bergstrom and P. Singer, Phys. Lett. **169B**, 297 (1986); P. Singer, Phys. Rev. **D42**, 3255 (1990).
- [7] Ya.I. Kogan and M.A. Shifman, Sov. J. Nucl. Phys. **38**, 628 (1983).
- [8] Review of Particles Properties, Phys. Rev. **D50**, August 1994.
- [9] I.F. Albuquerque *et al.*, Phys. Rev. **D50**, R18 (1994).
- [10] G. Eilam, A. Ioannissian, R.R. Mendel and P. Singer, preprint Technion-PH-95-18, hep-ph/9507267.
- [11] M.A. Shifman, A.I. Vainshtein and V.I. Zakharov, Nucl. Phys. **B147**, 385 (1979); **B147**, 448 (1979).
- [12] I.I. Balitsky *et al.*, Nucl. Phys. **B312**, 509 (1989).
- [13] C. Goldman and C.O. Escobar, Phys. Rev. **D 40**, 106 (1989).
- [14] A.J. Buras, M. Misiak, M. Munz and S. Pokorski, Nucl. Phys. **B424**, 374 (1994).
- [15] T. Inami and C.S. Lim, Prog. Theor. Phys. **65**, 297 (1981).
- [16] See also G. Burdman, E. Golovich, J.L. Hewett and S. Pakvasa, SLAC-PUB-6692, hep-ph/9502329 and referecens therein.
- [17] M.A. Shifman, A.I. Vainshtein and V.I. Zakharov, Phys. Rev. **D18**, 2583 (1978).
- [18] L.J. Reinders, H. Rubinstein ans S. Yazaki, Phys. Rep. **127**, 1 (1985).
- [19] For a more complete expansion see, for instance, K.-C. Yang et al., Phys. Rev. **D47**, 3001 (1993).
- [20] B.L. Ioffe and A.V. Smilga, Nucl. Phys. **B216**, 373 (1983); Phys. Lett. **B147**, 353 (1982).
- [21] I.I. Balitsky, V.M. Braun and A.V. Kolesnichenko, Yad. Fiz. **44**, 1582 (1986) [Sov. J. Nucl. Phys. **44**, 1028 (1986)].
- [22] B.L. Ioffe and A.V. Smilga, Phys. Lett. **B133**, 436 (1983).
- [23] D. Espriu and R. Tarrach, Nucl. Phys. **B214**, 285 (1983).
- [24] M.A. Shifman, A.I. Vainshtein and V.I. Zakharov, Nucl. Phys. **B120**, 316 (1977).
- [25] F.J. Gilman and M.B. Wise, Phys. Rev. **D20**, 2392 (1979).
- [26] B. Guberina and R.D. Peccei, Nucl. Phys. **B163**, 289 (1980).

## TABLES

TABLE I. Values of  $F_2$  and  $|\lambda_i|F_2$  for different internal quarks.

## FIGURES

FIG. 1. Typical diagrams contributing to hyperon radiative decays at quark level.

FIG. 2. Diagrams considered for the calculation of the Wilson coefficients of the correlator function. The crossed circle indicates the weak transition, with photon emission, and the cross on the s-quark line indicates that the  $m_s$  correction to the propagator is relevant.

FIG. 3. A  $q\bar{q}$  pair in the vacuum coupled to the electromagnetic current at large distances.

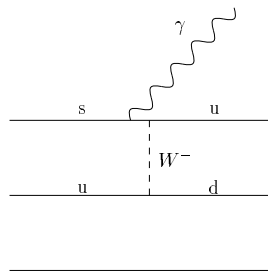
FIG. 4. The amplitude  $a_1$  as a function of  $M_1^2$  for  $M_2^2 = M_\Omega^2$  (full line),  $M_2^2 = 2.4\text{GeV}^2$  (dashed line) and  $M_2^2 = 3.2\text{GeV}^2$  (dotted line).

FIG. 5. The amplitude  $a_1$  as a function of  $M_2^2$  for  $M_1^2 = M_\Xi^2$  (full line),  $M_2^2 = 1.4\text{GeV}^2$  (dashed line) and  $M_2^2 = 2.0\text{GeV}^2$  (dotted line).

FIG. 6. Same as Figure 4 for  $b_1$ .

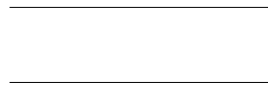
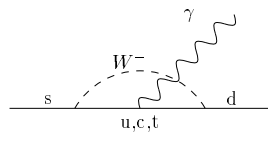
FIG. 7. Same as Figure 5 for  $b_1$ .

Quark	$F_2$	$ \lambda_i F_2$
u	$2.3 \times 10^{-9}$	$4.8 \times 10^{-10}$
c	$2.0 \times 10^{-4}$	$4.2 \times 10^{-5}$
t	0.39	$(4.7 - 28) \times 10^{-5}$

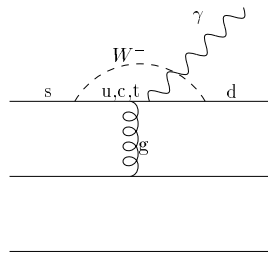


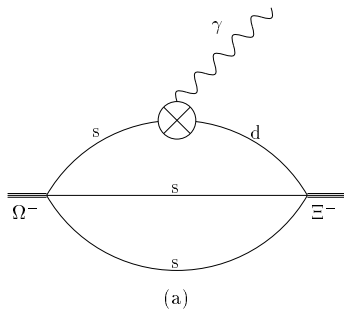
(a)

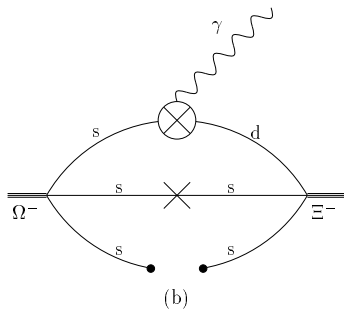


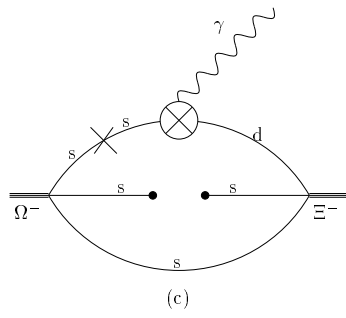


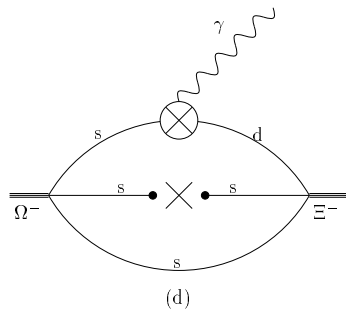
(b)

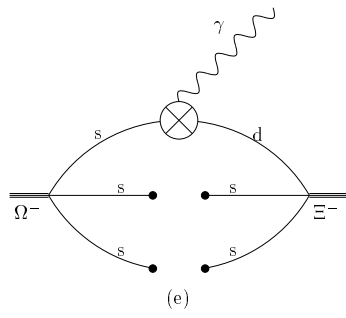


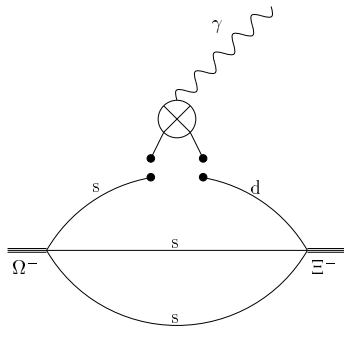






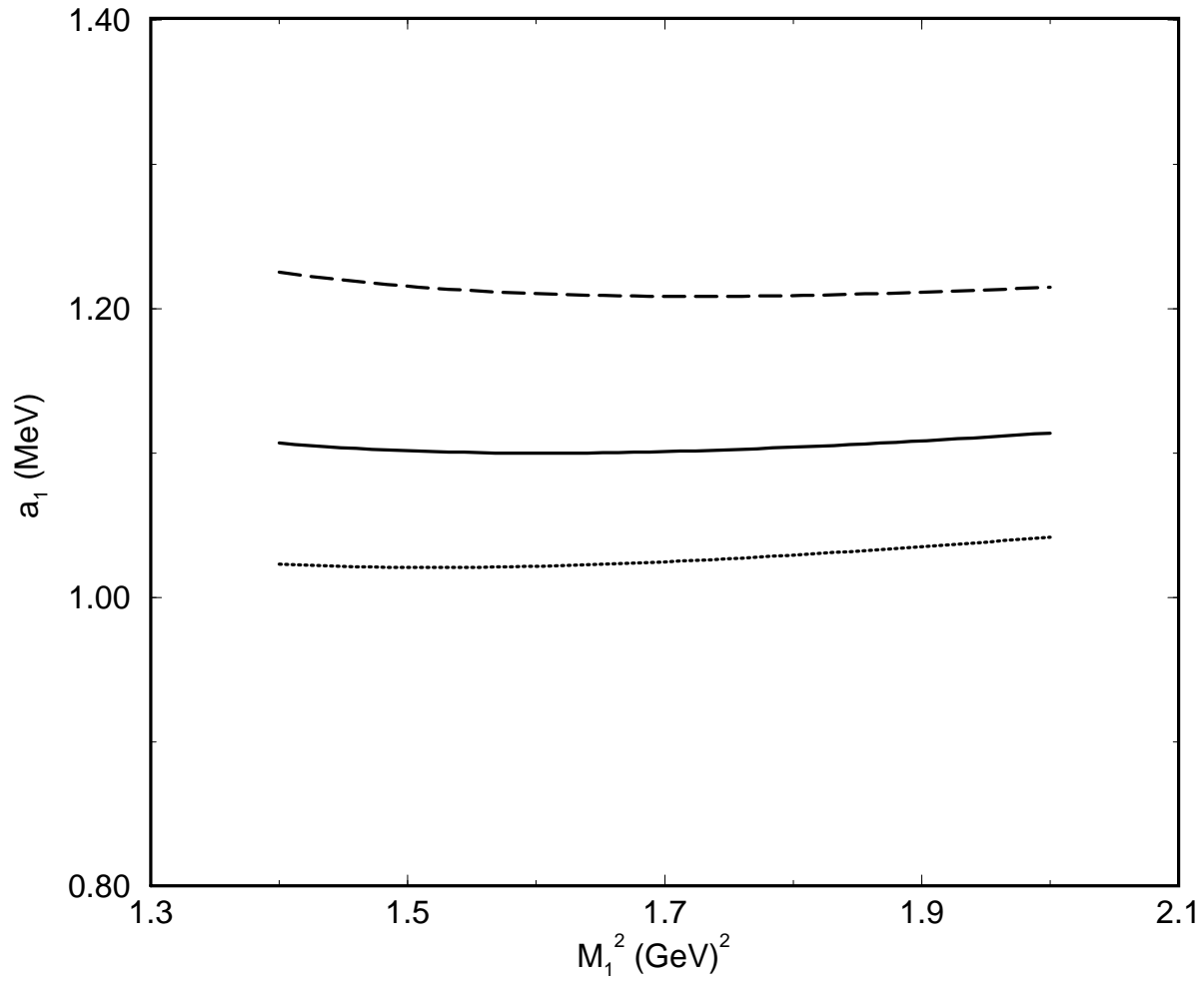








10



11

